Published in final edited form as:
*Reproduction*. 2009 February ; 137(2): 321–331. doi:10.1530/REP-07-0469.

# Oocyte-specific deletion of complex and hybrid N-glycans leads to defects in preovulatory follicle and cumulus mass development

**Suzannah A. Williams**[1] and **Pamela Stanley**[*]
Department of Cell Biology, Albert Einstein College of Medicine, New York, NY-10461, U.S.A.

## Abstract

Complex and hybrid N-glycans generated by N-acetylglucosaminyltransferase I (GlcNAcT-I), encoded by *Mgat1*, affect the functions of glycoproteins. We have previously shown that females with oocyte-specific deletion of a floxed *Mgat1* gene using a ZP3*Cre* transgene produce fewer pups due primarily to a reduction in ovulation rate. Here we show that the ovulation rate of mutant females is decreased due to aberrant development of preovulatory follicles. After a superovulatory regime of 48 h pregnant mare's serum (PMSG) and 9 h human chorionic gonadotropin (hCG), mutant ovaries weighed less and contained ~60% fewer preovulatory follicles and more atretic and abnormal follicles than controls. Unlike controls, a proportion of mutant follicles underwent premature luteinization. In addition, mutant preovulatory oocytes exhibited gross abnormalities with ~36% being blebbed or zona-free. While 97% of wild type oocytes had a perivitelline space at the preovulatory stage, ~54% of mutant oocytes did not. The cumulus mass surrounding mutant oocytes was also smaller with a decreased number of proliferating cells compared to controls, although hyaluronan around mutant oocytes was similar to controls. In addition, cumulus cells surrounding mutant eggs were resistant to removal by either hyaluronidase or incubation with capacitated sperm. Therefore, the absence of complex and hybrid N-glycans on oocyte glycoproteins leads to abnormal folliculogenesis resulting in a decreased ovulation rate.

### Keywords

*Mgat1*; GlcNAcT-I; N-glycans; oocyte; follicle; cumulus cells; premature luteinization

## Introduction

The development of a functional oocyte from the primordial to ovulatory stage, takes ~3 weeks in female mice (Pedersen & Peters 1968; Peters 1969) or potentially longer as observed in rats (Hirshfield 1989). Each oocyte develops within a follicle which provides the appropriate environment for oogenesis. Each follicle develops independently of gonadotropins, from recruitment as a meiotically-quiescent, primordial follicle through folliculogenesis to the late preantral stage when follicle stimulating hormone (FSH) is required. Luteinizing hormone (LH) stimulates preovulatory follicle development, oocyte maturation and ovulation. The oocyte, despite being meiotically-quiescent throughout folliculogenesis until ovulation, has an active role in the development of the follicle. It is now clear that there is considerable oocyte-follicle communication that is essential for successful oogenesis, and that the oocyte carefully

*Corresponding author: Telephone: 1-718-430-3346; Fax: 1-718-430-8574; stanley@aecom.yu.edu.
[1]Present address: Department of Physiology, Anatomy and Genetics, Le Gros Clark Building, University of Oxford, South Parks Road, Oxford, OX1 3QX, U.K.

**Declaration of Interest**
S.A.W. and P.S. declare no conflict of interest.

regulates the surrounding environment (Gilchrist, *et al.* 2004; Hutt & Albertini 2007; Matzuk, *et al*. 2002).

We have previously shown that female mice with a conditional *Mgat1* gene deletion which precludes the synthesis of hybrid and complex N-glycans solely in oocytes, have decreased fertility due to a decreased ovulation rate, and compromised preimplantation embryonic development (Shi, *et al*. 2004). Hybrid and complex N-glycans are generated following the addition of N-acetylglucosamine (GlcNAc) by N-acetylglucosaminyltransferase I (GlcNAcT-I) to $Man_5GlcNAc_2Asn$ at certain N-X-S/T sites in glycoproteins (Fig. 1). Mutant oocytes were generated by females carrying a floxed *Mgat1* gene and a ZP3*Cre* transgene (Shi *et al.* 2004). ZP3 is expressed from the primary stage of folliculogenesis (Philpott, *et al.* 1987), 2–3 weeks prior to ovulation. Females with no complex or hybrid N-glycans on oocyte glycoproteins produce litters ~50% smaller than controls. The decline in litter size is primarily due to a decrease in the number of eggs ovulated (Shi *et al.* 2004). The remaining reduction in fertility is due to aberrant preimplantation development in embryos generated from *Mgat1*$^{F/F}$:ZP3*Cre* females. While about half the embryos generated by fertilization of mutant eggs develop aberrantly, ~50% of these resume development upon implantation (Shi *et al*. 2004). The resumption of normal development demonstrates that the aberrant embryonic development during blastogenesis is not due to parthenogenic activation, or penetration of the modified mutant zona and fertilization by multiple sperm, because both of these events are lethal (Findlay, *et al*. 2007; Kono, *et al*. 2004; Sun 2003). Therefore, although complex and hybrid N-glycans are not essential for oogenesis, fertilization or preimplantation embryonic development, they play functional role(s) in oogenesis and ovulation.

In this paper we show that follicles with oocytes lacking complex and hybrid N-glycans have aberrant preovulatory follicular development, reflected in reduced numbers of preovulatory follicles, morphological abnormalities and premature luteinization. Mutant oocytes are also surrounded by a reduced number of proliferating cumulus cells and generate eggs with a small cumulus mass.

## Results

### Reduced ovulatory response in oocytes lacking complex and hybrid N-glycans

To determine if the decreased ovulation rate of *Mgat1*$^{F/F}$:ZP3*Cre* females reported previously (Shi *et al*. 2004) is due to aberrant development of preovulatory follicles or impaired ovulation, the number of ovarian follicles was determined in ovaries collected from females treated with PMSG for 48 h followed by hCG for 9 h. Mutant ovaries from unstimulated females were the same weight as control ovaries (Table 1). However, the weights of ovaries collected from *Mgat1*$^{F/F}$:ZP3*Cre* females after the superovulatory regime were less than control ovaries (Table 1). To identify all preovulatory follicles, every unstained section from one Bouin's-fixed ovary from each mouse was examined by light microscopy. Mutant ovaries were found to contain significantly fewer preovulatory follicles than control ovaries (20.0 ± 2.6 per control ovary (n=3) versus 8.2 ± 2.7 per mutant ovary (n=5), $P<0.001$).

To determine the stage at which folliculogenesis was modified in *Mgat1*$^{F/F}$:ZP3*Cre* females, follicles were counted and staged in every 15$^{th}$ section of the same Bouin's-fixed ovaries after staining with hematoxylin and eosin (H&E). Follicles were counted if the oocyte nucleus was visible, and preovulatory follicles were counted if the oocyte was clearly visible. Follicles were defined as normal, atretic or otherwise abnormal. The decrease in ovary weight in *Mgat1*$^{F/F}$:ZP3*Cre* females was reflected in a 58% decrease in the number of normal preovulatory follicles (controls: 15.7 ± 2.5 (n=3), mutant: 6.6 ± 2.9 (n=5)). Mutant ovaries contained fewer follicles in all categories compared to controls (Table 2). Interestingly, ~2 luteinizing follicles were present in each mutant ovary (n=5), whereas none were observed in

control ovaries (n=3) (Fig. 2B–C). The luteinizing granulosa cells of these follicles were larger and disorganized with the most luteinized cells being furthest from the oocyte (Fig. 2B'–C'). The percent of normal preovulatory follicles versus atretic/abnormal preovulatory follicles in *Mgat1* mutants was significantly different to controls (Table 2; $P<0.0001$, Chi-squared test). Overall 27% of mutant follicles were lost from the growing pool by atresia or premature luteinization compared to 8% of control follicles.

## Morphological analysis of preovulatory follicles with an oocyte lacking complex and hybrid N-glycans

Abnormalities of preovulatory follicles in *Mgat1* mutant ovaries that were clearly not luteinizing or undergoing atresia were common. In thin sections of glutaraldehyde-fixed mutant ovaries, the second ovary obtained from the same mice as the Bouin's-fixed ovaries analyzed in Table 2, oocytes had misshapen zona pellucidae, cumulus cells were observed beneath the zona and there were oocytes separated from their zona (Fig. 3A–D). To quantify the abnormalities, sections through the centre of oocytes of preovulatory follicles from the Bouin's-fixed ovaries were stained with hematoxylin and periodic acid Schiff reagent (H&PAS) and examined. Since mutant ovaries contained less preovulatory follicles (5–11), an equivalent number of preovulatory follicles per control ovary (10–11 randomly selected) were selected for further analysis. Preovulatory follicles were classified as grossly abnormal if they contained blebbed or disintegrating oocytes, oocytes lacking a zona and/or cumulus mass, or oocytes with cumulus cells present beneath the zona (Fig. 3E–J). *Mgat1* mutant follicles exhibited >3 times the number of gross abnormalities compared to controls (Fig. 3K).

## Additional abnormalities in follicles with an Mgat1$^{-/-}$ oocyte

The preovulatory follicles not classified as grossly abnormal in Fig. 3 were analysed further for PAS-positive vesicles, perivitelline space morphology, and cumulus mass size. *Mgat1*$^{-/-}$ preovulatory oocytes lacking hybrid and complex N-linked glycans contained large vesicles that reacted with the PAS reagent compared to the much smaller vesicles present in control oocytes (Fig. 4). PAS reacts with sugars and stains glycogen, zona proteins and other glycoproteins.

All preovulatory follicles classed as normal in Fig. 3 were classified into one of 4 categories according to the morphology of the perivitelline space between the zona and the oocyte (Fig. 5A). The perivitelline space was either: 1) continuous and completely surrounded the oocyte; 2) a continuous space spanning ~50% of the oocyte circumference; 3) discontinuous spaces surrounding the oocyte; or 4) absent. The vast majority of control oocytes were surrounded by a perivitelline space, either continuous or discontinuous. However ~50% of *Mgat1* mutant oocytes lacked any evidence of a perivitelline space (Fig. 5B). Therefore, the distribution of *Mgat1* mutant oocytes in each of the 4 categories was significantly altered compared to controls ($P<0.0001$; Chi-squared test). The transzonal processes (TZPs) connecting the oocyte and granulosa cells were visualized using transmission electron microscopy (Fig. 6A–D). The number of TZPs in mutant follicles was decreased compared to controls (Fig. 6E).

## Expansion of the cumulus mass matrix

The cumulus mass surrounding the oocyte in Bouin's-fixed preovulatory follicles not classed as grossly abnormal in Fig. 3 appeared to be smaller in ovaries from *Mgat1*$^{F/F}$:ZP3*Cre* females. Although a range in cumulus mass size was observed in both control and mutant ovaries, the three largest masses in mutant ovaries were clearly smaller than controls (Fig. 7A–F). To determine if the cumulus mass was smaller due to a decrease in cell number, proliferating cumulus cells in Bouin's-fixed preovulatory ovarian sections detected by an antibody to proliferating cell nuclear antigen (PCNA) were counted (Fig. 7G–I). The number of PCNA-

positive cells was significantly reduced in cumulus masses surrounding *Mgat1*$^{-/-}$ oocytes compared to controls (Fig. 7J).

To investigate the ability of cumulus cells surrounding mutant oocytes to undergo expansion, hyaluronan was examined by detection with hyaluronan binding protein (HABP) in Bouin's-fixed preovulatory follicles classed as normal in Fig. 3. Hyaluronan is secreted by cumulus cells in response to stimulation by the oocyte and is essential for cumulus expansion. HABP staining intensity of the cumulus mass surrounding *Mgat1*$^{-/-}$ oocytes was equivalent to control oocytes at a range of concentrations of HABP (Fig. 8A–E and data not shown). HABP staining also revealed the size of the expanded extracellular matrix surrounding the oocyte. *Mgat1* mutant cumulus masses were significantly smaller than wild type (Fig. 8F–G). To ensure that the reduced diameter of the *Mgat1* mutant extracellular cumulus mass was not due to lack of a perivitelline space, the width of the cumulus matrix was measured. This was also reduced in *Mgat1* mutant follicles (Fig. 8H–I). Therefore, oocytes lacking complex and hybrid N-glycans stimulate hyaluronan secretion by cumulus cells, but the reduced number of proliferating cumulus cells surrounding mutant oocytes contributes to a decrease in the size of the cumulus mass of preovulatory oocytes.

### Cumulus mass of ovulated eggs

Cumulus masses surrounding ovulated *Mgat1* mutant eggs were also smaller demonstrating that the developmental defect visible in the ovary did not preclude ovulation nor being collected by the fimbria into the oviduct (Fig. 9A–B). The smaller cumulus mass around ovulated *Mgat1*$^{-/-}$ eggs also indicates that cumulus modification occurring in the oviduct was not able to compensate for their decreased size. Furthermore, the cumulus complex that joined ovulated *Mgat1* mutant eggs together was thinner compared to controls (Fig. 9C–D).

The modified cumulus of *Mgat1* mutant eggs was also reflected in the finding that cumulus cells adjacent to the oocyte were resistant to removal by incubation with hyaluronidase (Shi *et al*. 2004). To determine if these cumulus cells could be removed by sperm which contain multiple hyaluronidases and arylsulfatase A that have a role in cumulus dispersal (Kim, *et al*. 2005; Miller, *et al*. 2007; Reitinger, *et al*. 2007; Wu, *et al*. 2007), ovulated eggs were incubated with capacitated sperm. Even after 4 h of co-incubation many of the cumulus cells surrounding *Mgat1*$^{-/-}$ eggs remained attached compared to the absence of virtually all cumulus cells on control eggs (Fig. 9E–F). Cumulus cells resistant to hyaluronidase were also not detached by calcium chelation using media containing EDTA or by decreasing the pH (data not shown). Therefore, despite hyaluronan being present in normal amounts, the cumulus cells on mutant eggs were resistant to removal by purified hyaluronidase and sperm.

### Cumulus cell attachment to the ZP

Since cumulus cells attached to the zona of *Mgat1*$^{-/-}$ oocytes were resistant to removal by hyaluronidase, sperm, EDTA and low pH, it was possible that they were attached by stray zona protein as occurs in ZP1 null females (Rankin, *et al*. 1999). However, scanning electron microscopy (SEM) revealed the surface of *Mgat1* mutant zona pellucida to be similar to wild type in appearance (Fig. 10A–C) despite the fragile, thin nature of the zona (Shi *et al*. 2004). These images also show that the resistance of cumulus cells to removal from *Mgat1*$^{-/-}$ eggs was not due to being retained by stray zona protein (Fig. 10A–C).

## Discussion

Oocyte-specific deletion of the *Mgat1* gene causes a decrease in eggs ovulated and fertility (Shi *et al*. 2004). We show here that the decrease in the number of ovulated eggs is due to aberrant folliculogenesis. Follicle numbers at all stages were reduced in *Mgat1* mutant ovaries.

A decrease in primary follicles was unexpected since the inactivation of the *Mgat1*gene occurs at this stage initiated by the expression of ZP3*Cre*, and therefore follicle recruitment was expected to be the same in mutant and control females. It is possible that abnormal mutant follicles at later stages affect the initial recruitment of follicles. In fact, this may also be the basis of the variation in the number of antral follicles observed after treatment with PMSG alone. We previously reported that mutant and control ovaries had the same number of antral follicles at 48 h after PMSG treatment (Shi *et al*., 2004). However, further analysis of additional mice revealed that, although the average did not differ between 9 mutant and 8 control ovaries (data not shown), the variation in antral follicle number amongst mutant ovaries was large, precluding a definitive conclusion.

Despite the number of abnormal preovulatory follicles, follicles containing mutant oocytes do develop, respond to hCG, attain preovulatory status and ovulate. These mutant eggs have a smaller cumulus cell mass with a reduced number of cumulus cells. However, this decreased size is not due to grossly abnormal secretion of hyaluronan, indicating that the signaling pathways that stimulate the secretion of hyaluronan are fully functional in oocytes with glycoproteins that lack complex and hybrid N-glycans. On the other hand, a proportion of follicles undergo premature luteinization, a phenomenon not commonly seen in controls. This indicates that the signals that originate from the oocyte and prevent granulosa cells undergoing luteolysis are modified.

The morphology of large antral follicles in *Mgat1*$^{F/F}$:ZP3*Cre* females does not differ from controls except for the generation of a thinner zona pellucida (Shi *et al*. 2004). However we show here that there were ~3.5-fold more abnormal preovulatory follicles in mutant compared to control ovaries. Therefore it appears that the later stages of follicular development are more sensitive to the absence of complex and hybrid N-glycans since numerous abnormalities were apparent 9 h after treatment with hCG. The response to the preovulatory LH surge is initiated by secretion from the mural granulosa cells of EGF ligands that stimulate EGF receptors on cumulus cells (Ashkenazi, *et al*. 2005; Park, *et al*. 2004). This induces the retraction of TZPs from the oocyte by the cumulus cells, resumption of meiosis by the oocyte, germinal vesicle breakdown and the expression of extracellular matrix proteins required for cumulus expansion by the cumulus cells. However, although oocyte maturation is triggered by the surge of LH from the pituitary, many of the subsequent maturation events are stimulated by the oocyte. Therefore, since the later stages of follicle development are defective in *Mgat1* mutants, these data identify a role for complex or hybrid N-glycans on oocyte glycoproteins at these stages and in cumulus expansion. The synthesis of these N-glycans is initiated in the medial Golgi, and thus the folding and chaperone functions of N-glycans necessary for exit of glycoproteins from the endoplasmic reticulum and progression along the secretory pathway, are not affected by the *Mgat1* mutation.

The oocyte plays an active role in the development of the follicle that surrounds and nurtures it (Gilchrist *et al*. 2004; Hutt & Albertini 2007; Matzuk *et al*. 2002). Growth differentiation factor-9 (GDF-9) is an oocyte-specific glycoprotein (McPherron & Lee 1993) with N-linked glycans (Elvin, *et al.* 1999). Mice lacking GDF-9 are infertile with follicles unable to develop beyond the primary stage (Dong, *et al*. 1996). GDF-9 functions synergistically with bone morphogenetic protein-15 (BMP-15) (Yan, *et al*. 2001) - another oocyte-specific glycoprotein (Dube, *et al*. 1998; Hashimoto, *et al*. 2005). Mice lacking BMP-15 have decreased fertility, but fertility is decreased further if the females are also heterozygous for GDF-9 and these females have cumulus expansion defects (Yan *et al*. 2001). Therefore, GDF-9 and BMP-15, being oocyte-specific glycoproteins involved in cumulus expansion, are potential candidates for giving rise to the *Mgat1* mutant phenotype. However, GDF-9 induces cumulus cells to express hyaluronan which is required for cumulus expansion, (Elvin *et al*. 1999), and hyaluronan is present in equivalent amounts in *Mgat1* mutant follicles to controls. This

indicates that GDF-9 and BMP-15 signaling is functional and thus GDF-9 and BMP-15 are unlikely to be responsible for the *Mgat1* mutant phenotype. However, the incidence of premature luteinization may indicate that the Smad4 signalling pathway has been affected by the loss of complex N-glycans from oocytes in some follicles since this also occurs in ovaries with a granulosa cell conditional deletion in Smad4 (Pangas *et al*. 2006). Cumulus cell differentiation is determined by proximity to the oocyte and the resulting gradient of influence (Diaz *et al*. 2007). Therefore the increased amount of luteinization furthest from the oocyte might reflect a defect in the prevention of luteinization by the oocyte.

The LH surge also stimulates the retraction of TZPs. TZPs are microtubules that extend from cumulus cells adjacent to the zona, penetrate through the zona pellucida and terminate on the oocyte joining the two cells (Anderson & Albertini 1976). TZPs communicate with the oocyte via gap junctions comprised of connexin-37 (Cx-37) expressed by the oocyte (Veitch, *et al*. 2004). Cx-37 is not glycosylated and therefore could not have a direct role in the *Mgat1* mutant phenotype. However, it has been shown that communication between the oocyte and cumulus cells regulates meiotic maturation of the oocyte (De La Fuente & Eppig 2001). Therefore, the cumulus cells adjacent to the zona that cannot be removed by hyaluronidase on *Mgat1* mutant oocytes may still be linked to the oocyte via TZPs. This connection could alter oocyte maturation and the later stages of follicular development and may be involved in the *Mgat1* mutant phenotype.

Many *Mgat1* mutant follicles also lack a perivitelline space. After the LH surge, the TZPs, as extensions of cumulus cells, secrete extracellular matrix proteins required for cumulus expansion which contribute to the generation of the perivitelline space (Talbot & Dandekar 2003). The lack of a perivitelline space around some *Mgat1* mutant oocytes could be due in part to the decrease in their TZPs. Furthermore, since the normal morphology of TZPs from mutant oocytes is modified, perhaps they are also not being appropriately retracted and are attaching the zona tightly to the surface of the oocyte. This could explain the resistance of cumulus cells to removal by hyaluronidase. Half the *Mgat1* mutant preovulatory follicles lack a perivitelline space and half the embryos generated from oocytes lacking complex N-glycans have aberrant preimplantation development (Shi *et al*. 2004). This correlation may indicate that the generation of a perivitelline space may be required for normal preimplantation embryogenesis. Indeed, the ability of an oocyte to form a perivitelline space has been linked with meiotic competence (Inoue, *et al*. 2007).

The large PAS-positive vesicles in *Mgat1*$^{-/-}$ oocytes indicate aberrant secretion of glycoproteins. Identification of oocyte glycoprotein(s) responsible for the defects seen in *Mgat1* mutants may be confounded due to the altered morphology of the zona pellucida. The *Mgat1* mutant zona is thin and fragile but *does* contain all three ZP proteins (Shi *et al*. 2004). It seems unlikely that the thickness of the mutant zona on *Mgat1*$^{-/-}$ eggs contributes to the aberrant oogenesis and embryonic development observed in *Mgat1* mutants since ZP1 null mice generate a thin zona but ovulate normal numbers of eggs (Rankin *et al*. 1999), and mice heterozygous for ZP3 generate a 50% thinner zona but fertility is unaffected (Wassarman, *et al*. 1997). However, it is possible that the altered structure of the *Mgat1* mutant zona has a modified function and may contribute, perhaps by limiting TZP abundance or release, to the compromised state of *Mgat1*$^{-/-}$ oocytes and/or ovulated eggs. Transmission electron microscopy revealed the decreased presence of TZPs in the mutant zona but does not reveal if the change in TZP quantity is due to modifications in TZP generation by oocyte glycoproteins or the structure of the modified zona. It also does not reveal if TZPs were released from mutant oocytes but remained trapped within the zona structure.

In summary, follicles containing oocytes lacking complex and hybrid N-glycans have defective follicle development leading to a significant decrease in preovulatory follicles and a decreased

ovulation rate. Most follicles with a mutant oocyte that continue development to become ovulatory do not generate a normal perivitelline space, a defect which has been linked to meiotic incompetence (Inoue, *et al*. 2007).

## Materials and Methods

### Mice

The mice were bred and maintained in the Institute for Animal Studies within the Albert Einstein College of Medicine. Female mice homozygous for a floxed *Mgat1* gene or heterozygotes with a floxed and null allele and carrying a ZP3*Cre* recombinase transgene in a 129/C57BL/6 mixed background (Shi *et al*. 2004) were used to generate oocytes lacking complex and hybrid N-glycans. Heterozygous $Mgat1^{F/-}$ females have no discernable phenotype (Shi *et al*. 2004). $Mgat1^{F/F}$ females lacking the ZP3*Cre* transgene were used as controls as we have shown that this transgene has no effect on fertility (Shi *et al*. 2004; Williams, *et al*. 2007).

### Hormonal stimulation protocol

To synchronize folliculogenesis or to obtain ovulated eggs, females were subjected to a superovulatory regime. Females were injected intraperitoneally with 5 IU of PMSG (Calbiochem, EMD Chemicals, Inc. San Diego, CA) followed after 46–48 h with 5 IU of hCG (Sigma, St. Louis, MO). Ovaries containing preovulatory follicles were collected 9 h after the hCG injection; all subsequent references to preovulatory follicles or ovaries refer to tissue collected after this treatment regime. Ovulated eggs were collected from the oviduct 14–16 h after the hCG treatment.

### Follicle morphology

To determine the number of preovulatory follicles, females were treated with PMSG for 48 h and ovaries collected 9 h after hCG administration. Female body and ovary weights were recorded. One ovary was fixed in Bouin's fixative and one in glutaraldehyde, as described below. The Bouin's ovary was fixed for ~12 h at room temperature followed by 3 washes of 5 min in 70% v/v EtOH, and an overnight wash in fresh 70% v/v EtOH at 4°C. Fixed ovaries were paraffin embedded, 3 μm serial sections were collected onto positively-charged slides and heated at 62°C for 1 h. Preovulatory follicles were counted in all unstained sections. To enable all follicle stages to be counted and staged, every 15th serial ovarian section (45 μm apart) was stained with hematoxylin and eosin (H&E) and analysed. All non-preovulatory follicles (primary: stages 3a and 3b; preantral: 4, 5a and 5b; antral: 6–8) in which the oocyte nucleus was visible were counted and staged according to Pedersen & Peters, 1968, including those morphologically atretic or abnormal. All preovulatory follicles where the oocyte, but not necessarily the nucleus, was clearly visible were counted and abnormalities noted.

Sections through the middle of Bouin's-fixed preovulatory follicle oocytes were selected for staining with H&PAS (Sigma), PAS-positive vesicle analysis, perivitelline space analysis, PCNA expression, and HABP analysis. Since mutant ovaries contained less preovulatory follicles as determined by counts of unstained sections, the number of control follicles stained with H&PAS for comparison to mutants was 10–11 per ovary, the maximum number found in a mutant ovary. To ensure control preovulatory follicles were chosen at random, the first 10–11 follicles identified were selected.

The second preovulatory ovary was fixed in 2.5% v/v glutaraldehyde in 0.1M sodium cacodylate for 1 h with agitation at room temperature, postfixed with 1% w/v osmium tetroxide followed by 1% uranyl acetate, dehydrated through a graded series of ethanol and embedded

in LX112 resin (LADD Research Industries, Burlington VT). Sections of 1 μm were cut on a Reichert Ultracut UCT and stained with 1% w/v Toluidine blue in 1% w/v sodium borate.

For transmission electron microscopy, ovaries from 5.5–10 week untreated mutant and control females were prepared as above. Ultrathin sections were cut on a Reichert Ultracut UCT, stained with uranyl acetate followed by lead citrate and viewed on a JEOL 1200EX transmission electron microscope at 80 kv. The TZPs were determined by measuring the area of the TZPs in the zona using NIH Image J. The image selected for TZP measurement contained the longest section of zona for each follicle.

### Proliferating cell nuclear antigen

To determine the number of proliferating cells in the cumulus matrix, sections through the centre of preovulatory oocytes were selected for PCNA staining. Bouin's-fixed, paraffin-embedded, 3 μm sections from ovaries of females treated with PMSG and hCG were dewaxed and rehydrated. Endogenous peroxidase was neutralized by incubating sections in 0.3% v/v $H_2O_2$ in methanol for 30 min at room temperature. Sections were washed twice for 5 min in phosphate buffered saline (PBS) before blocking background staining with 2% w/v bovine serum albumin (BSA)/PBS for ≥1 h at room temperature on a slow platform shaker. Sections were incubated with anti-PCNA antibody (P8825; Sigma) diluted at 1:200 in 2% BSA/PBS in a humidified chamber for ≥1 h at room temperature; controls were incubated in 2% BSA/PBS. Sections were washed for 3 min in PBS 3 times before incubating with a goat antibody to mouse IgG conjugated to horse radish peroxidase (Zymed) diluted 1/200 in 2% BSA/PBS in a humidified chamber for ≥1 h at room temperature. Sections were washed for 3 min in PBS 3 times before staining with 3,3'-diaminobenzidine using a peroxidase substrate kit (SK-4100; Vector Labs). The reagent was prepared according to manufacturer's instructions and all sections were exposed to the reagent for the same time within a single experiment before terminating the reaction by placing sections in distilled $H_2O$. The optimum reaction time for visualizing PCNA-positive cells was determined using a control section in each experiment. Sections were counter-stained with hematoxylin, dehydrated and mounted using Permount (Fisher).

### Detection of cumulus mass hyaluronan

Hyaluronan (hyaluronic acid) in the cumulus mass of preovulatory follicles was detected with hyaluronic acid binding protein (HABP) in paraffin-embedded ovary sections using immunofluorescence. Sections of 3 μm through the centre of preovulatory oocytes in Bouin's-fixed ovaries from females treated with PMSG and hCG were dewaxed and rehydrated before incubation in 3% BSA/PBS for ≥1 h with agitation at room temperature to block non-specific binding sites. Sections were incubated with ~100 μl diluted biotinylated HABP (400763-1; Seikagaku) at 0.5 μg/ml in 3% BSA/PBS for 2 h at room temperature; controls were incubated in 3% BSA/PBS. Sections were then washed in 3% BSA/PBS for 3 min at room temperature 3 times before incubation with 10 μg/ml HABP in 3% BSA/PBS Streptavadin Alexa Fluor @ 568 (Molecular Probes, Invitrogen) and incubated for 1 hour at room temperature. Sections were washed, mounted using Gel/Mount (Biomeda corp., Foster City, CA) and immediately photographed. To determine the size of the cumulus mass, photographs of preovulatory oocytes stained with HABP were printed. The diameter was determined from the average of 2 measurements taken perpendicular to each other across the centre of the oocyte. The width of the cumulus mass was the average of 4 measurements of the cumulus thickness at 4 equally spaced locations around the oocyte.

### Removal of cumulus cells by sperm

Females were treated with exogenous gonadotropins as described above and eggs were collected from oviducts into M2 media (Specialty Media, Phillipsburg, NJ) that had been

equilibrated overnight at 37°C 95% $CO_2$ 5% air. To obtain capacitated sperm, the cauda was dissected from C57BL/6 males and the sperm squeezed out into M2 media. Sperm were incubated for 15 min to allow dissemination, before counting at 4 μm on a Coulter counter. Sperm were added to equilibriated media at 1 million/ml and incubated for 1 h to allow them to undergo capacitation. Oviducts containing ovulated eggs were obtained from superovulated females and added to the capacitated sperm. Eggs were released and gametes co-incubated for 4 h at 37°C. At the end of the incubation period, eggs were transferred into separate dishes and photographed.

### Collection of eggs for scanning electron microscopy (SEM)

Oocytes with retained cumulus cells were examined by SEM. Females were injected intraperitoneally with 5 IU of PMSG followed 46 h later with 5 IU of hCG, and ovaries were collected after 9–12 h into Earle's buffered salt solution (Gibco) containing 0.1% w/v PVP (EBSS/PVP). The largest follicles were punctured using fine dissecting needles to release oocyte cumulus complexes (OCCs) into the medium. Ovulated OCCs were also used. OCCs collected from both follicles and oviducts were exposed to prolonged incubation (~20–30 min) in EBSS/PVP containing 0.3 mg/ml hyaluronidase (Sigma) and protease inhibitors (Roche, Indianapolis, IN). Oocytes were washed in EBSS/PVP before fixation in 2.5% glutaraldehyde in 0.1M sodium cacodylate for 1 h at room temperature with agitation, dehydrated through a graded series of ethanol, critical point dried using liquid carbon dioxide in a Tousimis Samdri 790 Critical Point Drier (Rockville MD), sputter coated with gold-palladium in a Denton Vacuum Desk-1 Sputter Coater (Cherry Hill NJ). Ovaries were imaged in a JEOL JSM6400 scanning electron microscope (Peabody MA), using an accelerating voltage of 10 KV. Images were recorded with AnalySIS, (Olympus Soft Imaging Systems GMBH).

### Statistical analysis

Counts of PCNA-positive cells, cumulus diameter and width measurements, and preovulatory follicle classification were carried out blinded. All values are mean ± STDEV. Values were analyzed by two-tailed unpaired *t*-tests using Microsoft Excel Data Analysis Package. Distribution of the percent of follicles in each category of perivitelline space and of the percent of healthy preovulatory follicles versus atretic/abnormal were analyzed using the Chi-squared test (http://www.graphpad.com/quickcalcs/chisquared2.cfm).

## Acknowledgments

We thank Wen Dong and Henry Kurniawan for excellent technical assistance, Radma Mahmood and Rani Sellers of the AECOM Histopathology Facility for advice and technical assistance, and the Analytical Imaging Facility for sectioning, Toluidine staining, SEM and TEM.

**Funding**

This work was supported by the National Institutes of Heath (RO1 30645 to P.S.) and partial support was provided by the Albert Einstein Cancer Center grant (PO1 13330).

## References

Anderson E, Albertini DF. Gap junctions between the oocyte and companion follicle cells in the mammalian ovary. The Journal of Cell Biology 1976;71:680–686. [PubMed: 825522]

Ashkenazi H, Cao X, Motola S, Popliker M, Conti M, Tsafriri A. Epidermal growth factor family members: endogenous mediators of the ovulatory response. Endocrinology 2005;146:77–84. [PubMed: 15459120]

De La Fuente R, Eppig JJ. Transcriptional activity of the mouse oocyte genome: companion granulosa cells modulate transcription and chromatin remodeling. Developmental Biology 2001;229:224–236. [PubMed: 11133166]

Diaz FJ, Wigglesworth K, Eppig JJ. Oocytes determine cumulus cell lineage in mouse ovarian follicles. Journal of Cell Science 2007;120:1330–1340. [PubMed: 17389684]

Dong J, Albertini DF, Nishimori K, Kumar TR, Lu N, Matzuk MM. Growth differentiation factor-9 is required during early ovarian folliculogenesis. Nature 1996;383:531–535. [PubMed: 8849725]

Dube JL, Wang P, Elvin J, Lyons KM, Celeste AJ, Matzuk MM. The bone morphogenetic protein 15 gene is X-linked and expressed in oocytes. Molecular Endocrinology 1998;12:1809–1817. [PubMed: 9849956]

Elvin JA, Clark AT, Wang P, Wolfman NM, Matzuk MM. Paracrine actions of growth differentiation factor-9 in the mammalian ovary. Molecular Endocrinology 1999;13:1035–1048. [PubMed: 10379900]

Findlay JK, Gear ML, Illingworth PJ, Junk SM, Kay G, Mackerras AH, Pope A, Rothenfluh HS, Wilton L. Human embryo: a biological definition. Reproduction 2007;22:905–911.

Gilchrist RB, Ritter LJ, Armstrong DT. Oocyte-somatic cell interactions during follicle development in mammals. Animal Reproduction Science 2004;82–83:431–446.

Hashimoto O, Moore RK, Shimasaki S. Posttranslational processing of mouse and human BMP-15: potential implication in the determination of ovulation quota. Proceedings of the National Academy of Sciences of the United States of America 2005;102:5426–5431. [PubMed: 15809424]

Hirshfield AN. Granulosa cell proliferation in very small follicles of cycling rats studied by long-term continuous tritiated-thymidine infusion. Biology of Reproduction 1989;41:309–316. [PubMed: 2804222]

Hutt KJ, Albertini DF. An oocentric view of folliculogenesis and embryogenesis. Reproductive Biomedicine Online 2007;14:758–764. [PubMed: 17579993]

Inoue A, Akiyama T, Nagata M, Aoki F. The perivitelline space-forming capacity of mouse oocytes is associated with meiotic competence. The Journal of Reproduction and Development 2007;53:1043–1052. [PubMed: 17587772]

Kim E, Baba D, Kimura M, Yamashita M, Kashiwabara S, Baba T. Identification of a hyaluronidase, Hyal5, involved in penetration of mouse sperm through cumulus mass. Proceedings of the National Academy of Sciences of the United States of America 2005;102:18028–18033. [PubMed: 16330764]

Kono T, Obata Y, Wu Q, Niwa K, Ono Y, Yamamoto Y, Park ES, Seo JS, Ogawa H. Birth of parthenogenetic mice that can develop to adulthood. Nature 2004;428:860–864. [PubMed: 15103378]

Matzuk MM, Burns KH, Viveiros MM, Eppig JJ. Intercellular communication in the mammalian ovary: oocytes carry the conversation. Science 2002;296:2178–2180. [PubMed: 12077402]

McPherron AC, Lee SJ. GDF-3 and GDF-9: two new members of the transforming growth factor-beta superfamily containing a novel pattern of cysteines. The Journal of Biological Chemistry 1993;268:3444–3449. [PubMed: 8429021]

Miller KA, Shao M, Martin-DeLeon PA. Hyalp1 in murine sperm function: evidence for unique and overlapping functions with other reproductive hyaluronidases. Journal of Andrology 2007;28:67–76. [PubMed: 16928892]

Pangas SA, Li X, Robertson EJ, Matzuk MM. Premature luteinization and cumulus cell defects in ovarian-specific Smad4 knockout mice. Molecular Endocrinology 2006;20:1406–1422. [PubMed: 16513794]

Park JY, Su YQ, Ariga M, Law E, Jin SL, Conti M. EGF-like growth factors as mediators of LH action in the ovulatory follicle. Science 2004;303:682–684. [PubMed: 14726596]

Pedersen T, Peters H. Proposal for a classification of oocytes and follicles in the mouse ovary. Journal of Reproduction and Fertility 1968;17:555–557. [PubMed: 5715685]

Peters H. The development of the mouse ovary from birth to maturity. Acta Endocrinologica 1969;62:98–116. [PubMed: 5394354]

Philpott CC, Ringuette MJ, Dean J. Oocyte-specific expression and developmental regulation of ZP3, the sperm receptor of the mouse zona pellucida. Developmental Biology 1987;121:568–575. [PubMed: 2884155]

Rankin T, Talbot P, Lee E, Dean J. Abnormal zonae pellucidae in mice lacking ZP1 result in early embryonic loss. Development 1999;126:3847–3855. [PubMed: 10433913]

Reitinger S, Laschober GT, Fehrer C, Greiderer B, Lepperdinger G. Mouse testicular hyaluronidase-like proteins SPAM1 and HYAL5 but not HYALP1 degrade hyaluronan. The Biochemical Journal 2007;401:79–85. [PubMed: 16925524]

Shi S, Williams SA, Seppo A, Kurniawan H, Chen W, Ye Z, Marth JD, Stanley P. Inactivation of the *Mgat1* gene in oocytes impairs oogenesis, but embryos lacking complex and hybrid N-glycans develop and implant. Molecular and Cellular Biology 2004;24:9920–9929. [PubMed: 15509794]

Sun QY. Cellular and molecular mechanisms leading to cortical reaction and polyspermy block in mammalian eggs. Microscopy Research and Technique 2003;61:342–348. [PubMed: 12811739]

Talbot P, Dandekar P. Perivitelline space: does it play a role in blocking polyspermy in mammals? Microscopy Research and Technique 2003;61:349–357. [PubMed: 12811740]

Veitch GI, Gittens JE, Shao Q, Laird DW, Kidder GM. Selective assembly of connexin37 into heterocellular gap junctions at the oocyte/granulosa cell interface. Journal of Cell Science 2004;117:2699–2707. [PubMed: 15138288]

Wassarman PM, Qi H, Litscher ES. Mutant female mice carrying a single mZP3 allele produce eggs with a thin zona pellucida, but reproduce normally. Proceedings. Biological Sciences / The Royal Society 1997;264:323–328. [PubMed: 9107049]

Williams SA, Xia L, Cummings RD, McEver RP, Stanley P. Fertilization in mouse does not require terminal galactose or N-acetylglucosamine on the zona pellucida glycans. Journal of Cell Science 2007;120:1341–1349. [PubMed: 17374637]

Wu A, Anupriwan A, Iamsaard S, Chakrabandhu K, Santos DC, Rupar T, Tsang BK, Carmona E, Tanphaichitr N. Sperm surface arylsulfatase A can disperse the cumulus matrix of cumulus oocyte complexes. Journal of Cellular Physiology 2007;213:201–211. [PubMed: 17474085]

Yan C, Wang P, DeMayo J, DeMayo FJ, Elvin JA, Carino C, Prasad SV, Skinner SS, Dunbar BS, Dube JL, Celeste AJ, Matzuk MM. Synergistic roles of bone morphogenetic protein 15 and growth differentiation factor 9 in ovarian function. Molecular Endocrinology 2001;15:854–866. [PubMed: 11376106]

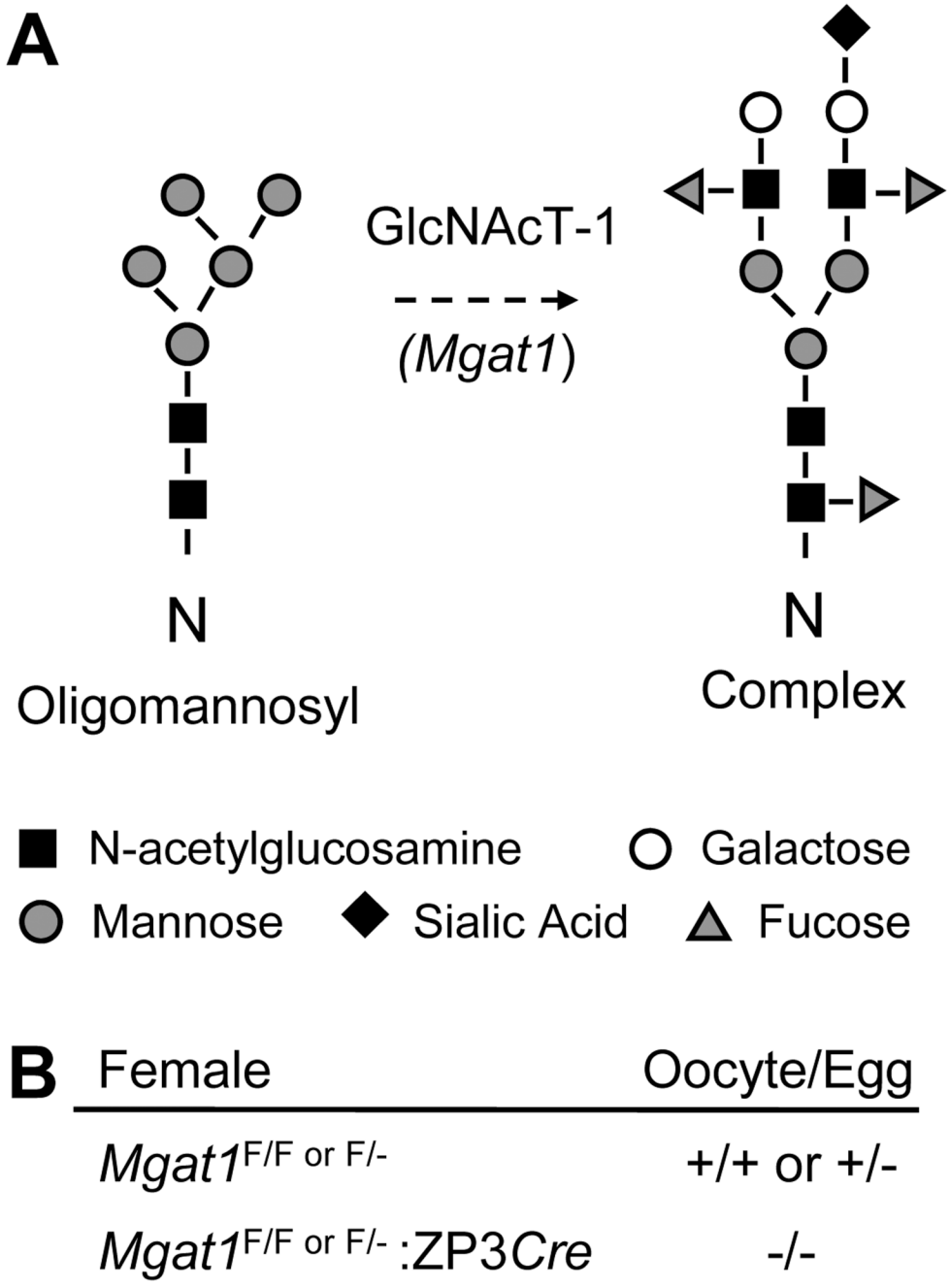


**Figure 1.**
(A) The oligomannosyl substrate of GlcNAcT-I which is encoded by the *Mgat1* gene, and a complex N-glycan whose synthesis is initiated by the action of GlcNAcT-I. (B) Genotype of female mice and their oocytes. F = floxed.

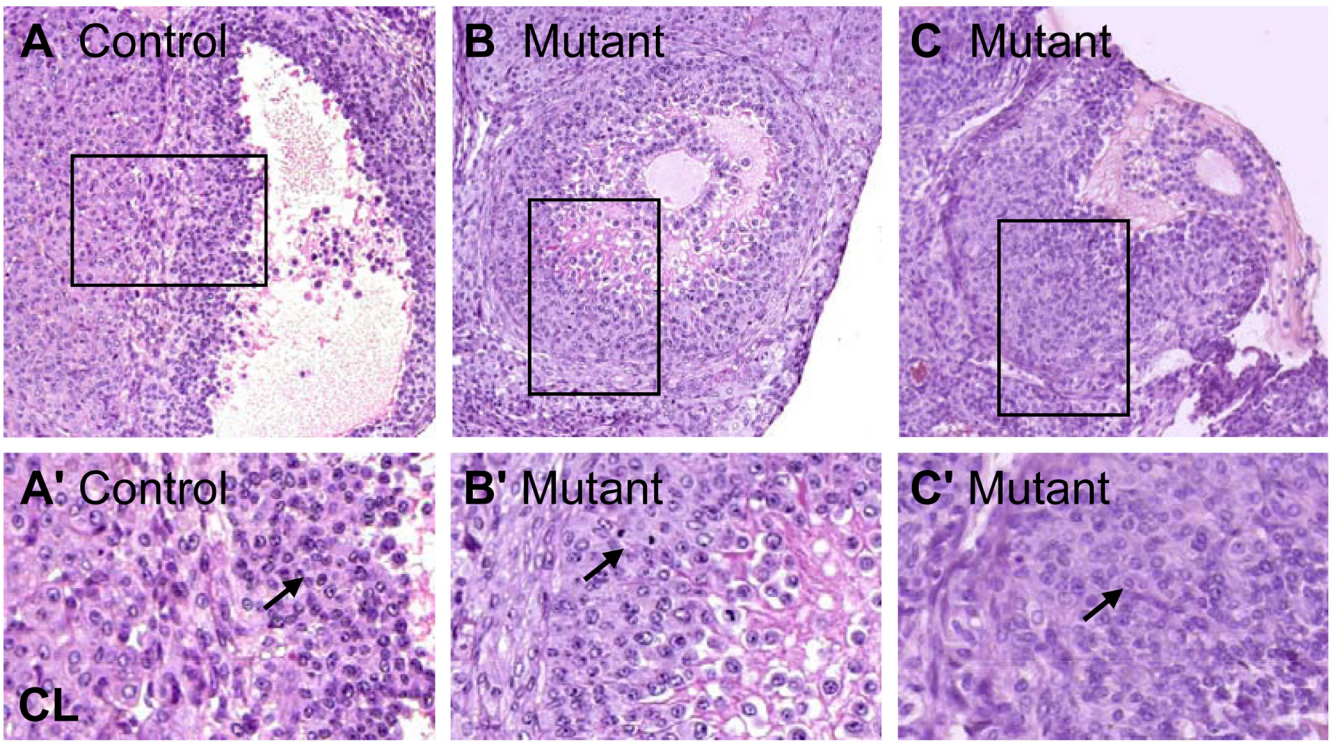


**Figure 2.**

Abnormal premature luteinization of granulosa cells in *Mgat1* mutant follicles. Sections are from preovulatory mouse ovaries after a superovulatory regime by administration of PMSG followed 48 h later by hCG stimulation with ovary collection at 57 h. Sections stained with H&E were from ovaries analyzed in Table 2. (A) Control preovulatory follicle adjacent to a CL. (B) Mutant preovulatory follicle containing partially-luteinized granulosa cells. (C) Mutant preovulatory follicles containing luteinized granulosa cells. (A'–C') The area marked by each square in A–C is magnified. Images are at the same magnification and the same exposure and are rotated when necessary. (A') Granulosa cells of a control preovulatory follicle (arrow) and the border with a CL. (B') Partially-luteinized granulosa cells (arrow) of preovulatory *Mgat1* mutant follicles. (C') Luteinized cells (arrow) of preovulatory mutant follicles.

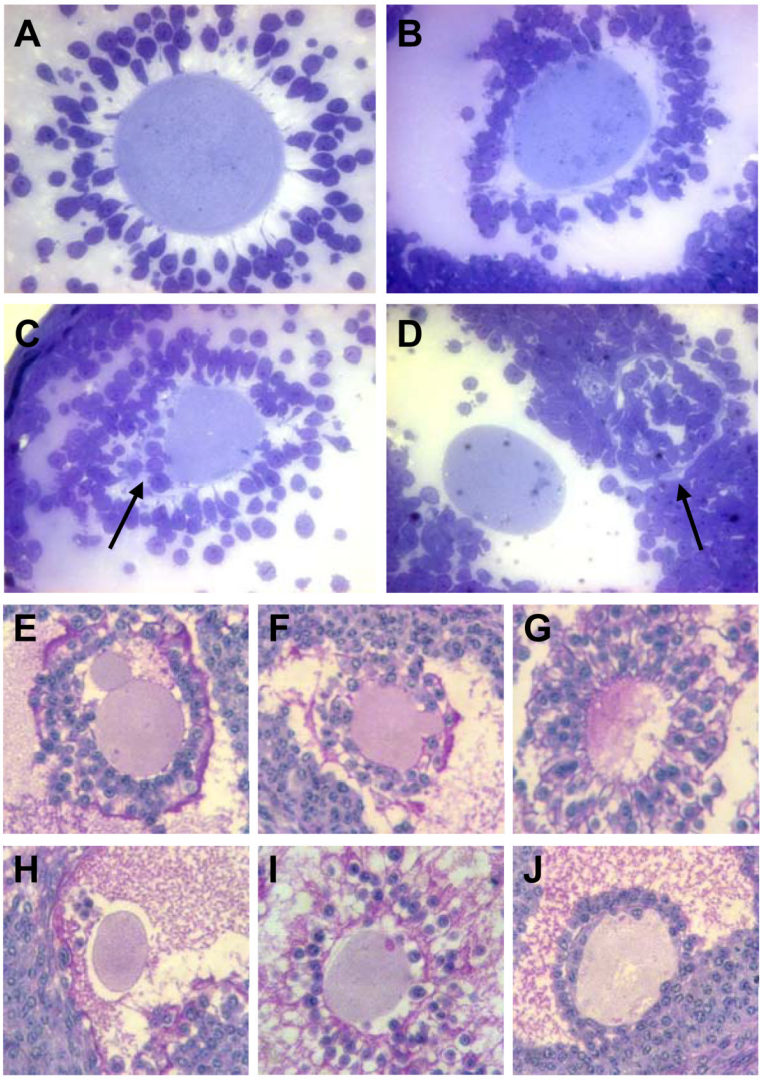


K

| | Control | Mutant |
|---|---|---|
| Total preovulatory follicles examined (No. females) | 32 (n=3) | 42 (n=5) |
| % grossly abnormal oocytes/female | 9.7 ± 10.0 | 36.1 ± 2.9* |

**Figure 3.**

Morphology of the zona pellucida in mouse preovulatory follicles. (A–D) Ovaries from females treated with PMSG and hCG were fixed in glutaraldehyde, sectioned (1 μm) and stained with Toluidine blue. (A) Preovulatory follicle in control ovary with thick ZP and large expanded cumulus cell mass. (B) Mutant oocyte with baggy zona pellucida and non-expanded cumulus mass. (C) *Mgat1* mutant oocyte with cumulus cells beneath the zona pellucida (arrow) and poorly expanded cumulus mass. (D) *Mgat1* mutant oocyte with a separate zona pellucida visible on the right (arrow). (E–J) Bouin's-fixed ovary sections were from the ovaries analyzed in Table 2. Sections through the centre of preovulatory follicle oocytes were selected and stained with H&PAS. (E) A grossly abnormal blebbed oocyte with cumulus cells present beneath the

zona of a mutant oocyte. (F) Blebbing oocyte with cumulus cells beneath the zona. (G) Disintegrating oocyte. (H) Oocyte with no zona or cumulus cell mass. (I–J) Invasive cumulus cells beneath the zona pellucida of a mutant oocyte. (K) Percent of oocytes with abnormalities (mean ± STDEV; *$P$=0.001). Images A–D and E–J are at the same magnification.

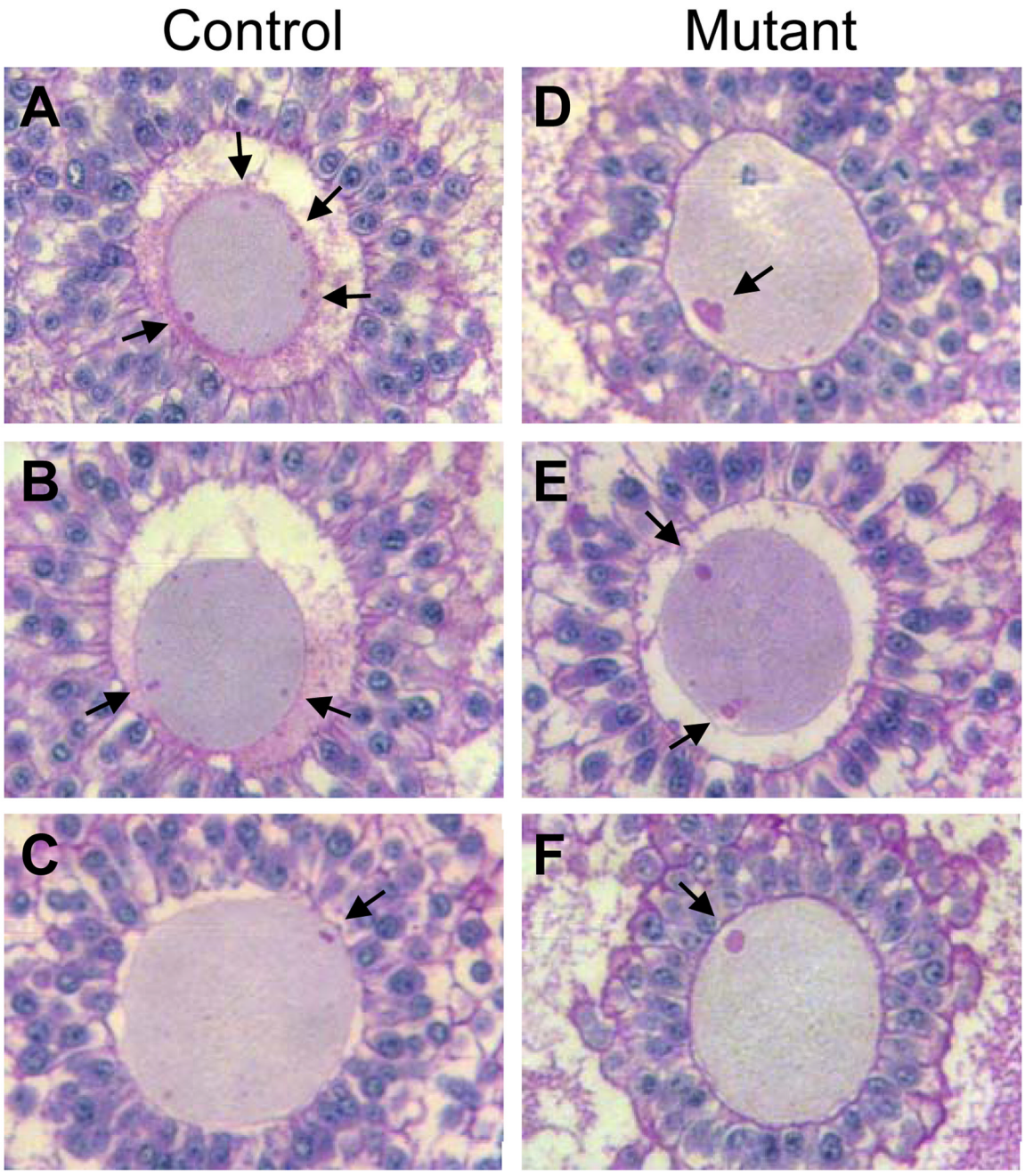


**Figure 4.**

*Mgat1* mutant mouse preovulatory oocytes contain large PAS-positive vesicles. (A–C) Control and (D–F) mutant oocytes not classified as grossly abnormal in Fig. 3 that contained PAS-positive vesicles (arrows). These oocytes represent those in each genotype with the largest PAS-stained vesicles from 29 control oocytes (n=3 females) and 28 mutant oocytes (n=5 females). Images are at the same magnification.

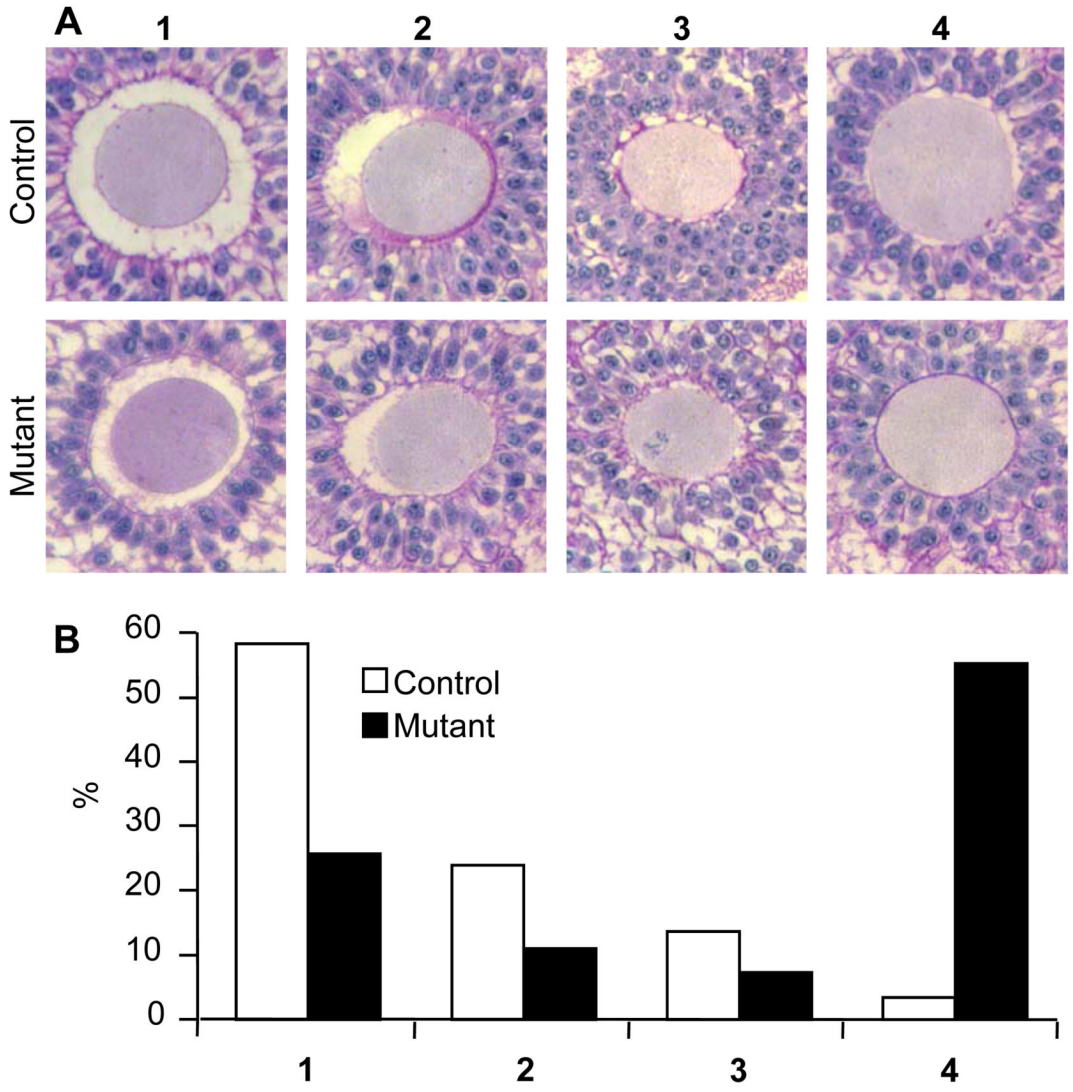


**Figure 5.**

The perivitelline space was decreased around *Mgat1* mutant preovulatory mouse oocytes. Sections through the centre of oocytes stained with H&PAS were selected from control and mutant follicles not classified as grossly abnormal in Fig. 3. (A1) Continuous perivitelline space, (A2) ~50% continuous perivitelline space, (A3) ~50% discontinuous perivitelline space, and (A4) no visible perivitelline space. (B) The distribution of follicles in each category was significantly different (control oocytes n=29, mutant oocytes n=28; $P<0.0001$). Images are at the same magnification.

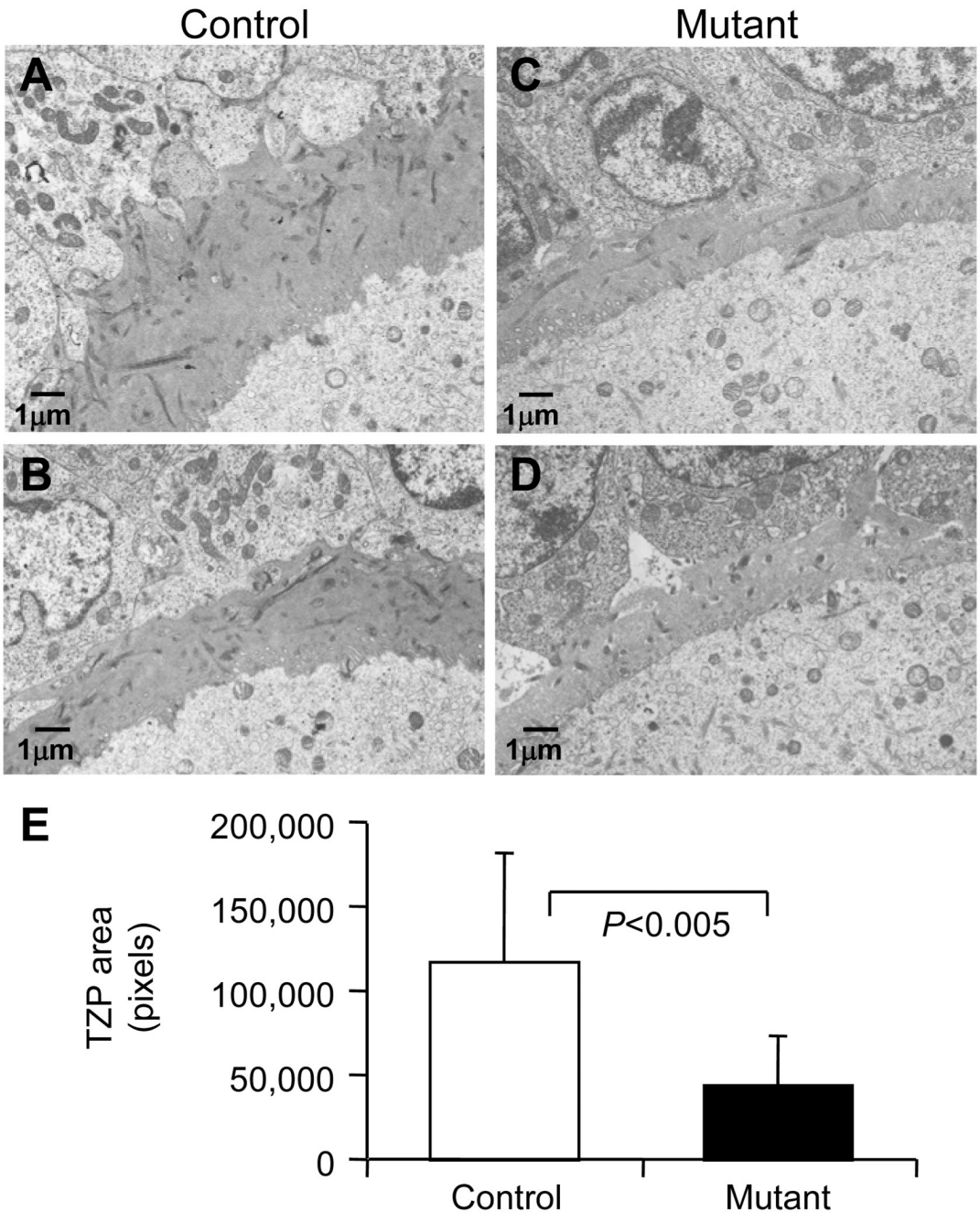


**Figure 6.**
Transmission electron microscopy visualization of transzonal processes (TZPs). Representative images of the zona of control (A–B) and mutant (C–D) follicles from untreated female mice. (E) The area of TZPs in the control and mutant sections (mean ± STDEV; control and mutant, n=13 follicles from 3 females each).

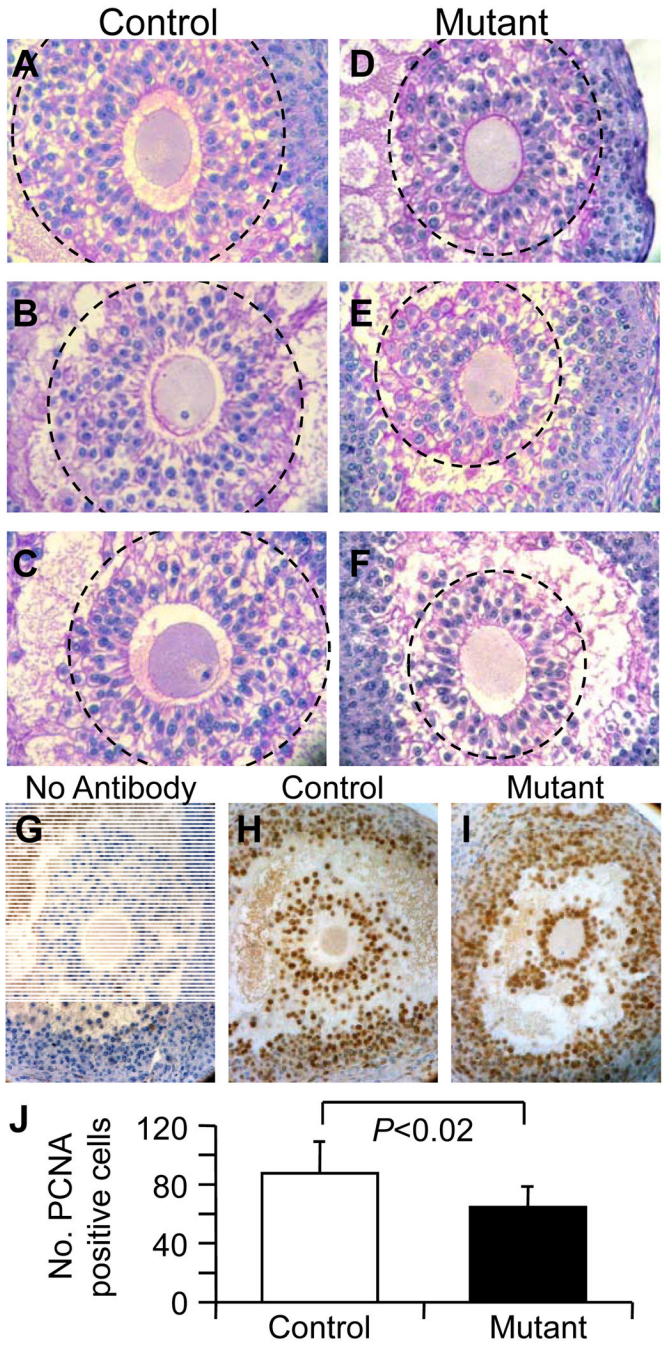


**Figure 7.**

The cumulus mass of preovulatory follicles was smaller in *Mgat1* mutant mouse ovaries. The 3 oocytes with the largest cumulus mass were selected from preovulatory ovarian follicles not classified as grossly abnormal in Fig. 3 (control (A–C) n=29; mutant (D–F), n=28). The cumulus mass contained reduced numbers of PCNA-positive (brown) cumulus cells in preovulatory follicles from *Mgat1* mutant ovaries. (G–I) PCNA staining of cumulus cells and blue hematoxylin counter staining. (J) Number of PCNA-positive cumulus cells (mean ± STDEV; control, n=6 follicles from 3 females; mutant, n=11 follicles from 5 females, 2–3 follicles per mouse). Images A–F and G–I are at the same magnification.

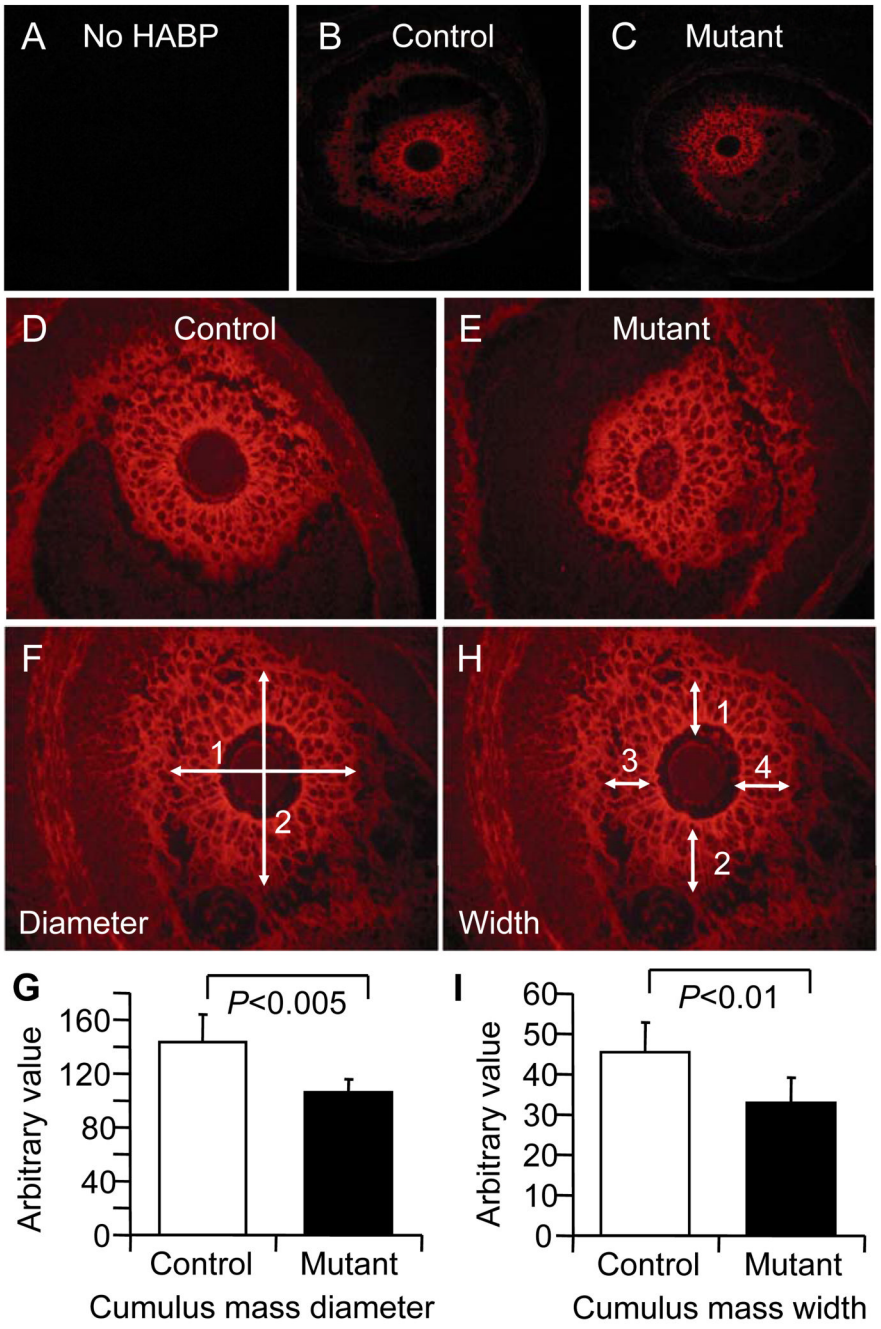


**Figure 8.**

Hyaluronan in expanded cumulus matrix of preovulatory follicles in mouse ovarian sections after PMSG and hCG stimulation. Sections through the centre of preovulatory follicle oocytes were selected from those follicles not classified as grossly abnormal in Fig. 3. (A–E) Intensity of HABP binding to the cumulus mass is equivalent in *Mgat1*$^{F/F}$:ZP3*Cre* ovaries compared to controls. Pictures are representative of 3 experiments using 8 control and 13 mutant sections. HABP binding revealed the cumulus matrix and the average diameter (F) and width (H) determined from photographs printed at the same magnification; the scale is arbitrary. (G) The diameter of the cumulus matrix and (I) the width were larger in control cumulus complexes

compared to those in follicles from *Mgat1* mutant ovaries (mean ± STDEV; control, n=6 from 3 females; mutant, n=7 from 4 females).

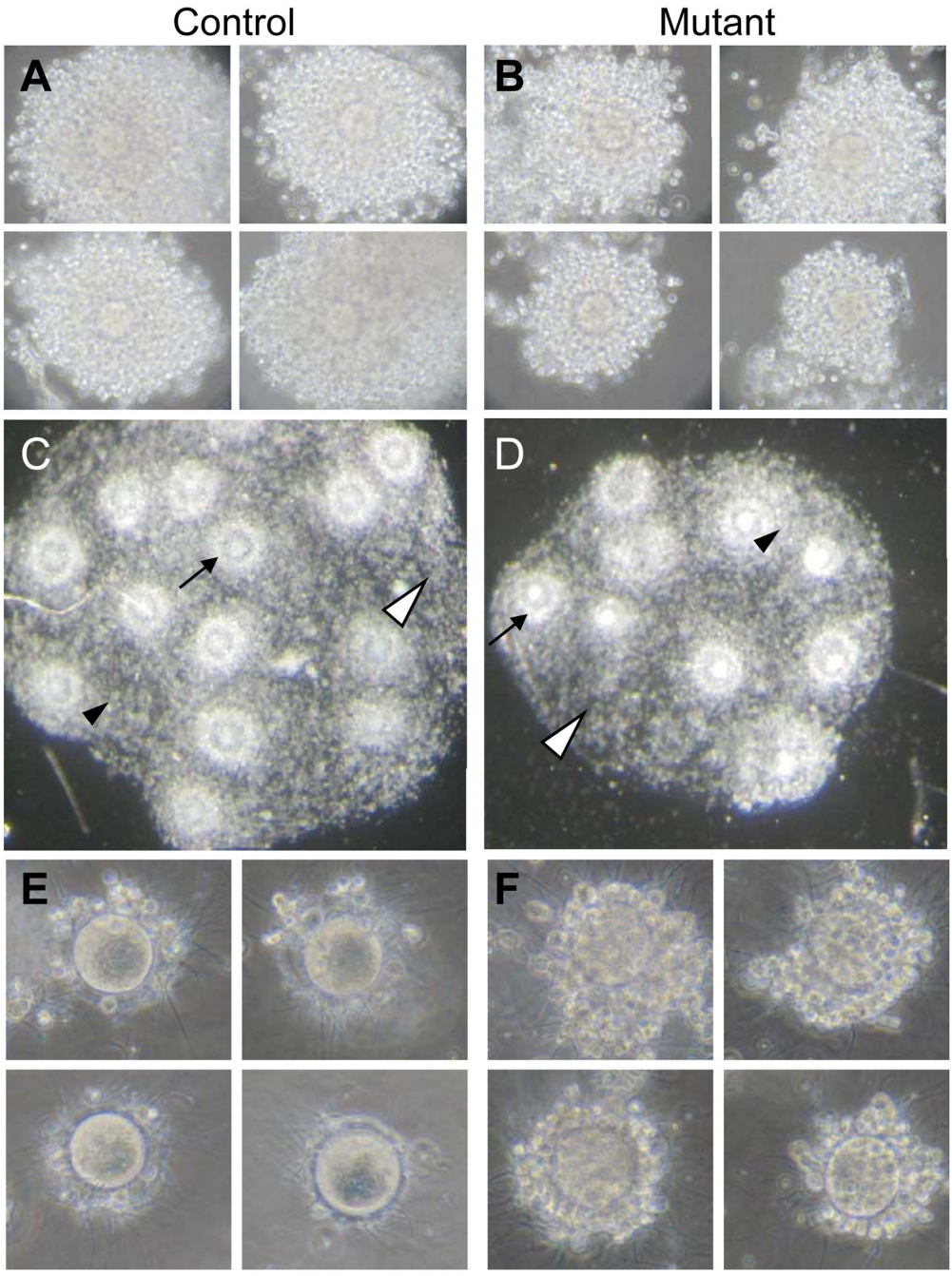


**Figure 9.**

Cumulus of ovulated eggs from superovulated control and *Mgat1*$^{F/F}$:ZP3*Cre* female mice. (A–B) The cumulus mass surrounding each mutant egg was smaller compared to control eggs. Representative of 19 control eggs from 6 females and 16 mutant eggs from 6 females. (C–D) The cumulus mass was larger and contained more eggs from control compared to *Mgat1*$^{F/F}$:ZP3*Cre* females. The cumulus mass matrix surrounding control and *Mgat1*$^{-/-}$ eggs was dense (black arrowheads) or sparse (white arrowheads). A space surrounding the egg was clearly evident in the majority of control eggs but rarely observed around *Mgat1*$^{-/-}$ eggs (arrows). Representative of 11 control and 11 mutant cumulus masses collected in 4 experiments. (E–F) Cumulus cells surrounding *Mgat1*$^{-/-}$ eggs are not only resistant to removal

by digestion with hyaluronidase (Shi *et al*. 2004) but also by *in vitro* incubation with sperm. Ovulated eggs were incubated with capacitated sperm for 4 hours. Representative of 21 control eggs collected from 7 females and 42 mutant eggs collected from 8 females in 2 experiments.

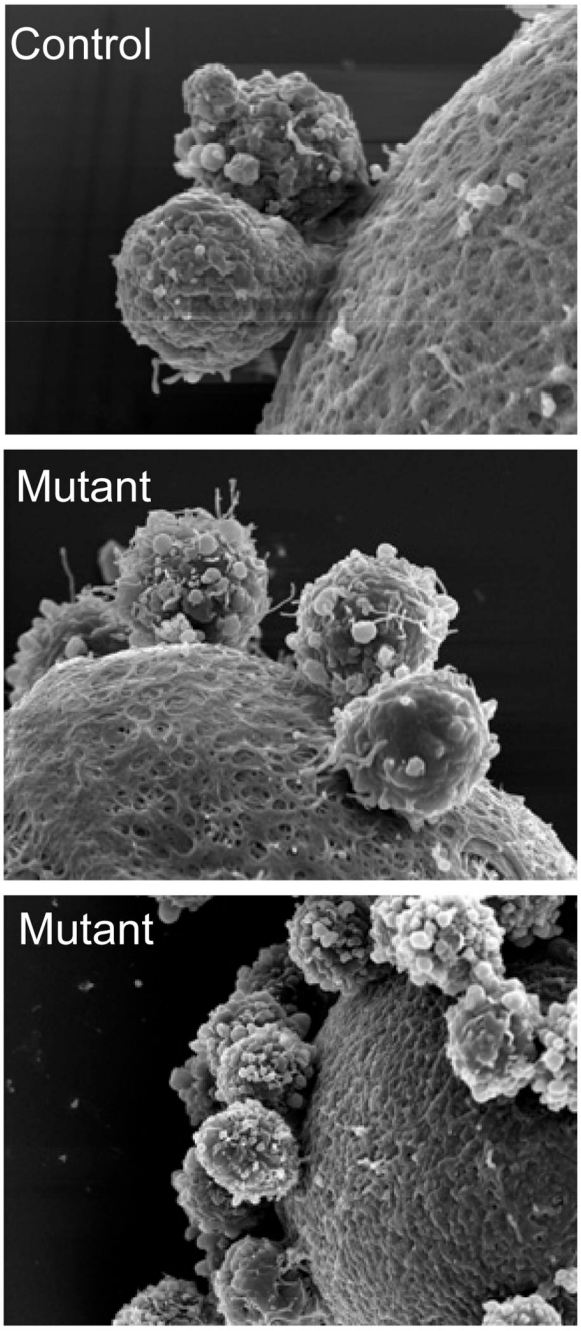


**Figure 10.**
Scanning electron micrographs of cumulus cells attached to the zona of *Mgat1*$^{-/-}$ mouse eggs. Scanning electron micrographs of cumulus cells attached to the zona of control and *Mgat1*$^{-/-}$ eggs showed that the cumulus cells were not retained on the zona enclosing *Mgat1*$^{-/-}$ eggs by stray zona pellucida.

## Table 1

Ovary weights from unstimulated and hormone-stimulated *Mgat1*$^{F/F}$:ZP3*Cre* and control female mice

| | | Control | Mutant |
|---|---|---|---|
| **Unstimulated**[a] | | n=4 | n=4 |
| | Body (g) | 18.2 ± 1.5 | 17.2 ±1.1 |
| | Ovary (mg) | 26.4 ± 7.5 | 27.9 ± 3.8 |
| **PMSG + hCG**[b] | | n=3 | n=5 |
| | Body (g) | 22.6 ± 1.7 | 22.2 ± 2.8 |
| | Ovary (mg) | 78.2 ± 16.0 | 56.9 ± 4.1* |

[a] 6.5 week littermates from 2 sets of parents;

[b] 7 week females from 4 sets of parents analyzed in Table 2. Values are mean ± STDEV.

* $P<0.05$.

**Table 2**

Follicle counts of *Mgat1*$^{F/F}$:ZP3*Cre* ovaries after hormone stimulation.

| | Primary | Preantral (% atretic) | Antral (% atretic/ abnormal) | Preovulatory (% atretic/ abnormal) | Total |
|---|---|---|---|---|---|
| **Control** (n=3) | 72.0 ± 13.5 | 43.7 ± 15.1 (8 ± 8) | 6.7 ± 3.8 (32 ± 16) | 17.0 ± 1.0 (8 ± 14) | 139.3 ± 31.8 |
| **Mutant** (n=5) | 49.4 ± 25.6 | 14.8 ± 5.8 (9 ± 6) | 2.8 ± 1.9 (37 ± 41) | 9.2 ± 3.3 (27 ± 21)* | 76.2 ± 24.5 |

Follicles were counted in one ovary per mouse collected at 57 h after administration of PMSG at 0 h and hCG at 48 h. Values are mean (± STDEV).

*Abnormal preovulatory follicles included luteinizing follicles and corpora lutea containing an oocyte.